RSC Advances

PAPER

View Article Online
View Journal | View Issue

Cite this: *RSC Adv.*, 2018, **8**, 20801

SOMC grafting of vanadium oxytriisopropoxide ($VO(O^iPr)_3$) on dehydroxylated silica; analysis of surface complexes and thermal restructuring mechanism†

Manuel P. Högerl,‡[a] Li Min Serena Goh,‡[a] Edy Abou-Hamad,[a] Samir Barman,[a] Oliver Dachwald,[b] Farhan Ahmad Pasha,[a] Jeremie Pelletier,[a] Klaus Köhler,[b] Valerio D'Elia,*[ac] Luigi Cavallo*[a] and Jean-Marie Basset*[a]

Received 20th March 2018
Accepted 30th May 2018

DOI: 10.1039/c8ra02419g

rsc.li/rsc-advances

Vanadium oxytriisopropoxide ($VO(O^iPr)_3$), **1**, was grafted on highly dehydroxylated silica ($SiO_{2\text{-}700}$: aerosil silica treated at 700 °C under high vacuum) to generate compound **2** following the concepts and methodology of surface organometallic chemistry (SOMC). The resulting compound was analyzed by elemental analysis, FT-IR, ^1H, ^{13}C and ^{51}V solid state (SS) NMR, Raman and EPR spectroscopies. The grafting reaction of **1** to generate **2** was found to lead to the formation of a monopodal surface complex $[(\equiv Si{-}O{-})V(O)(O^iPr)_2]$, **2m**, as well as bipodal $[(\equiv Si{-}O{-})_2V(O)(O^iPr)]$, **2b**, formed along with $(\equiv Si{-}O{-}^iPr)$ moieties as an effect of the classical rearrangement of **2m** with strained siloxane bridges. Upon controlled thermal treatment at 200 °C under high vacuum, **2m** and **2b** were found to mainly rearrange to tetrahedral VO_4 moieties $[(\equiv Si{-}O{-})_3V(O)]$ (**3**) with formation of propylene whereas the $(\equiv Si{-}O{-}^iPr)$ groups were preserved. The mechanism of the thermal rearrangement of the isopropoxide groups was investigated by a DFT approach revealing the occurrence of a concerted γ-H-transfer and olefin elimination mechanism.

Introduction

Vanadium oxo complexes on oxide supports have attracted the attention of researchers in the fields of catalysis and inorganic chemistry for their role in promoting the oxidation of organic compounds[1] and the non-oxidative[2] and oxidative[3] dehydrogenation of propane (ODHP) just to cite a few key applications. When employing traditional preparative techniques such as incipient wetness impregnation for the synthesis of supported vanadium oxo complexes, a distribution of monomeric and polymeric VO_x species is generally formed on the surface irrespective of precursor and support.[4–7] As an effect, it is difficult to characterize the individual surface domains and to evaluate their role in catalysis when using such materials.[3,8–16] Among relevant vanadium oxo complexes, vanadium(IV) isopropoxide species have been often indicated as key intermediates within the mechanism of ODHP:[17–19] the vanadium isopropoxide intermediate, formed after the first H-abstraction, should undergo a non-rate determining,[17,19] H-transfer to an oxygen atom (V–O-support or V=O) of the catalyst to generate propene before the catalytic cycle is completed by reoxidation of the V centers (Scheme 1).[18–26]

The experimental observation and isolation of vanadium isopropoxide species under the reaction conditions of conventional ODHP catalysis is extremely challenging because they are

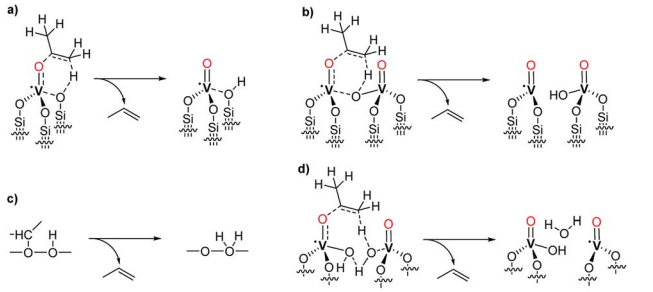

Scheme 1 Proton abstraction from V(IV) isopropoxide intermediates as proposed in several computational studies: (a) ref. 19, (b) ref. 18, (c) ref. 17, (d) ref. 20.

[a]*KAUST Catalysis Center, King Abdullah University of Science and Technology, 23955-6900 Thuwal, Saudi-Arabia. E-mail: Jeanmarie.basset@kaust.edu.sa; luigi.cavallo@kaust.edu.sa*

[b]*Departments of Chemistry and Catalysis Research Center, Technical University of Munich, Lichtenbergstrasse 4, Ernst-Otto-Fischer-Strasse 1, 85747 Garching, Germany*

[c]*Department of Materials Science and Engineering, School of Molecular Science and Engineering, Vidyasirimedhi Institute of Science and Technology (VISTEC), 21210, Payupnai, WangChan, Rayong, Thailand. E-mail: valerio.delia@vistec.ac.th*

† Electronic supplementary information (ESI) available: Experimental methods and details, additional IR spectra; computational coordinates and DFT energy diagram. See DOI: 10.1039/c8ra02419g

‡ These authors contributed equally.

labile intermediates formed after the rate determining step.[19] Furthermore, it is extremely challenging to prepare vanadium(IV) complexes with uniform structure and oxidation state as well-defined and isolated species on the support surface. A viable strategy for the study of the transformation of supported vanadium isopropoxide species is by the grafting of more stable V(V) oxo isopropoxide complexes and the study of their stoichiometric transformations.[27,28]

In this context, a recent contribution to the elucidation of the structure and of the chemical reactivity of silica-supported vanadium oxo isopropoxide species has been reported by Hermans *et al.* by grafting **1** on highly dehydroxylated silica.[28] The authors were able to show that, upon thermal treatment starting at 200 °C, the isolated [(≡Si–O–)V(O)(O^iPr)$_2$] complexes generated on the surface would undergo thermal restructuring leading to the formation of isolated tetrahedral VO_4 sites along with two molecules of propene.

Surface organometallic chemistry (SOMC) allows the synthesis and investigation of well-defined and isolated surface complexes by advanced preparative and diagnostic tools.[29,30] The grafting of suitable organometallic complexes by this strategy under rigorously controlled conditions is a useful tool for the preparation and the study of well-defined pre-catalytic complexes and supported reaction intermediates that could not be isolated by homogeneous organometallic chemistry.[31–34] For instance, we have recently shown that by employing highly dehydroxylated silica supports,[35] and by the careful application of SOMC-grafting techniques, it is possible to prepare truly isolated tetrahedral VO_4 units that show a higher propylene productivity compared to that of traditional impregnated catalyst applied under identical conditions.[36] This observation justifies the application of the advanced SOMC preparative tools for a more accurate study of vanadium oxo surface complexes related to the reaction network of ODHP.

Whereas, in previous studies, the grafting of **1** was carried out by the reaction of its vapors with silica,[27,28] this work, analyzes the apparently different (and differently distributed) complexes formed by the solution-phase grafting of **1** on $SiO_{2\text{-}700}$ by the SOMC protocol and the corresponding products of rearrangement after controlled thermolysis. Furthermore, given the lack of computational studies analyzing the reactivity of well-defined, supported vanadium(V) isopropoxide complexes, we applied density functional theory (DFT) calculations to gain deeper insights into the thermal restructuring of **2m**. The occurrence of a concerted step of γ-H-transfer and olefin elimination, rather than a two-step radical process, is shown in this stoichiometric transformation.

Experimental section

All experiments were carried out using Schlenk equipment or in Argon filled gloveboxes (<0.1 ppm H_2O, <0.1 ppm O_2), and by using high-vacuum lines (~10^{-5} mbar). Solvents were dried by use of a commercial solvent purification system (CuO catalysts/Alox) and degassed by two freeze–pump–thaw cycles. Molecular sieves were dried in vacuum 10^{-3} mbar for 12 h at 300 °C. Further information on analytical techniques and instrumentation is available in the ESI.†.

Partially dehydroxylated silica ($SiO_{2\text{-}700}$) was prepared by heat treatment of Evonik Aerosil 200 (10 g) under vacuum in a quartz tube. The starting silica material was pretreated with a minimal amount of water (~10 mL) to ease its handling and was dehydroxylated at 700 °C for 18 h under vacuum (~10^{-5} mbar).

Synthesis of 2

A mixture of [VO(O^iPr)$_3$], (purchased from Sigma-Aldrich as a clear, pale yellow solution; used as received because the analysis of the sample by liquid NMR gave no indication of decomposition or impurities) (0.080 mL) and $SiO_{2\text{-}700}$ (1 g) in pentane (10 mL) was stirred at r.t. overnight. After filtration, the solid (**2**) was washed 3 times with pentane and the liquid was transferred to a round bottom flask to quantify the isopropanol evolved during grafting by quantitative NMR using hexamethylbenzene C_6Me_6 as an internal standard. Analysis by NMR indicated the formation of 0.9 ± 0.1 isopropanol/V during grafting. The resulting white powder was dried under vacuum (~10^{-5} mbar).

Anal. found: V, 1.42; C, 2.02; H, 0.42 (%). ^{1}H MAS NMR (600 MHz): δ 5.5, 4.3, 1.4, and 1.2 ppm. ^{13}C CP-MAS NMR (600 MHz): δ 85, 67, and 23 ppm.

Thermolysis of 2 to 3

The thermolysis of **2** was carried out as a self-supporting silica pellet (~30–50 mg) in a custom made vacuum IR cell. Experiments were carried out under static or dynamic vacuum to continuously remove any gaseous product (~10^{-5} mbar). After the reaction time, the formed gases were (a) analyzed by transmission IR spectroscopy, and (b) sampled by gas-syringe from the reaction vessel and subjected to gas-chromatography, or (c) transferred to another vessel by trapping them with liquid N_2 and then sampled, or (d) evacuated.

Results and discussion

1 was reacted with silica (Aerosil® 200 from Evonik) partially dehydroxylated at 700 °C ($SiO_{2\text{-}700}$) in pentane to generate **2**. Elemental analysis of **2** revealed a vanadium loading of 1.42 ± 0.1 wt% suggesting an approximate average of 0.9 V-atoms per nm^2 (0.28 mmol V g^{-1}), which compares well with the number of available surface silanol groups (~ 1.0 per nm^2, 0.23–0.3 mmol silanol/g).[35] The C/V molar ratio of 6.0 (expected C/V ratio for **1**: 6) is in agreement with the presence of two isopropyl fragments per atom of vanadium.

Controlled thermolysis reaction of **2** (2 °C min^{-1} from ~23 to 200 °C, 1 h at 200 °C) as a self-supporting pellet under static vacuum conditions (~10^{-5} mbar) to generate **3** led to the formation of nearly stoichiometric amounts of propene in the gas phase, as observed by IR and GC/FID/MS (0.95 equiv. propene C_3H_6 per V, see the ESI (Fig. S1†)). Oxygenates, such as isopropanol and acetone, possible products of ligand dissociation and dehydrogenation, were observed only in trace amounts.

Grafting of **1** on $SiO_{2\text{-}700}$ led to the appearance of the ν(C–H) bands (at 2970–2878 cm^{-1}) and of the δ(C–H) bands (1467, 1453, 1384, 1371, 1326 cm^{-1}) of **1** in the FTIR spectrum (Fig. 1) of **2** with the concomitant nearly complete disappearance of the

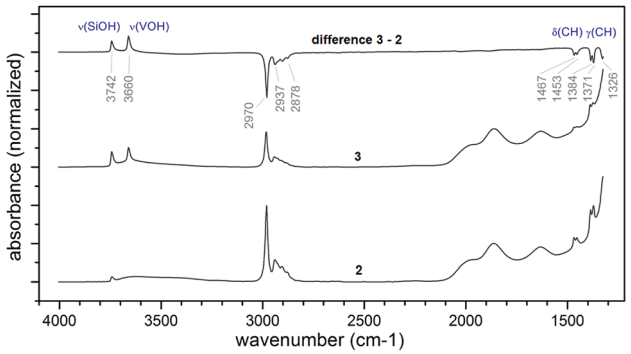

Fig. 1 IR spectra comparing the product of grafting of **1** (**2**, bottom trace), the material after thermolysis at 200 °C for 1 h (**3**, middle trace), and the difference spectrum of **2** and **3** (C, top trace).

ν(O–H) at 3741 cm^{-1} relative to the isolated silanols of the pristine support (see Fig. S2† for a comparison of **2** and $SiO_{2\text{-}700}$).[37] IR analysis before and after (**3**) the thermolysis reaction at 200 °C for 1 h under static vacuum showed a clear decrease of the intensity of the aliphatic bands present in **2**, with the concomitant formation of a new sharp band at 3660 cm^{-1} and the reappearance of the silanol band at 3742 cm^{-1} (Fig. 1). The band at 3660 cm^{-1} can be assigned to a ν(VO–H) stretching mode.[36,38]

Along with the 1 : 1 V/initial silanols ratio obtained from the elemental analysis of **2**, the nearly complete disappearance of the band relative to the isolated silanols, suggests that each precursor complex reacts stoichiometrically with a single silanol. To note, this result is different from what obtained by Hermans *et al.* when vapors of **1** were reacted with $SiO_{2\text{-}700}$. In that case, an excess of precursor reacted with the support leading to a vanadium loading of about 2.9 wt% (about the double as obtained in our case). The authors attributed this observation to the reaction of the precursor also with the strained siloxane bridges of $SiO_{2\text{-}700}$.[28]

Furthermore, the IR spectra in Fig. 1 show that upon thermal treatment of **2** at 200 °C, only part of the organic isopropyl groups, responsible for the signal at 2970–2878 cm^{-1}, are removed from the surface.

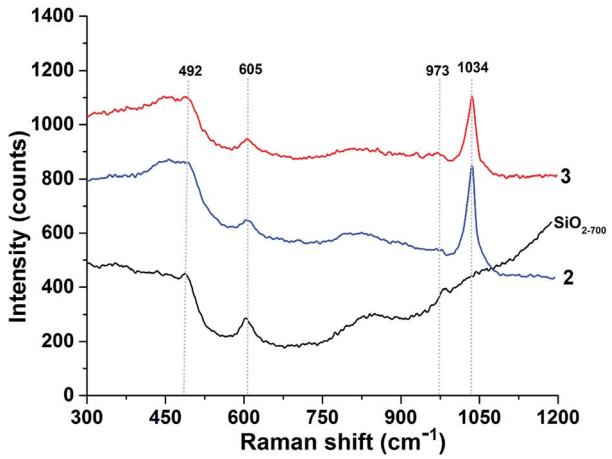

Fig. 2 Raman spectra of $SiO_{2\text{-}700}$, **2** and **3**.

Analysis of **2** and **3** by Raman spectroscopy (Fig. 2) shows that either before and after thermal treatment the vanadyl group is present in the samples as supported by the intense absorption band at 1030–1035 cm^{-1} attributable to the isolated vanadyls of **2** and **3**. The absence of bands in the 980–1000 cm^{-1} region excludes the formation of crystalline vanadia.[3,6]

To assess the oxidation state of the vanadium atoms before and after thermal treatment, **2** and **3** have been investigated by *in situ* electron paramagnetic resonance spectroscopy (EPR). In all cases, well-resolved EPR spectra of V(IV) were obtained with well resolved hyperfine structure (Fig. S3†). However, after careful quantitative calibration with standard V(IV) samples, it was found that the percentage of V(IV) relative to V(V) did not exceed 1.5% for **2**. Also, after treatment of **2** to generate **3**, the relation between V(IV) to V(V) did not exceed 2%. In addition, no indication of V(III) species was obtained at any stage. Therefore, the formation of paramagnetic V(IV) species, as observed by *in situ* EPR studies, was limited to a very minor component of **2** and **3**.

To assess the structure of **2** and **3** the ^{1}H and ^{13}C SS NMR spectra of these compounds were measured. The ^{1}H spin-echo MAS NMR spectrum of **2** shows four signals at 1.2, 1.4, 4.3, and 5.5 ppm (Fig. 3A). The signals at 1.2 and 1.4 ppm auto correlate in 2D Double-Quantum (DQ) and Triple-Quantum (TQ) ^{1}H–^{1}H homonuclear dipolar correlation spectra (Fig. 3B and C respectively) and were therefore assigned to the methyl groups of the two isopropoxide ligands of **2** in two slightly different chemical environments.

The proton resonances at 4.3 and 5.5 ppm display no auto-correlation in the DQ or TQ spectra, and were therefore assigned to C–H methine groups of isopropoxide ligands of **2** in two different chemical environments.

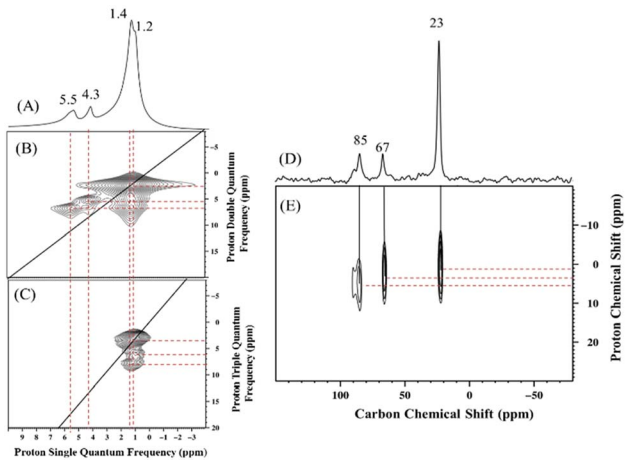

Fig. 3 Solid-state NMR spectra of **2** (A) 1D ^{1}H spin-echo MAS (20 kHz MAS, number of scans = 32, and repetition delay = 5 s) (B) 2D ^{1}H–^{1}H DQ (C) 2D ^{1}H–^{1}H TQ (22 kHz MAS, with a back-to-back recoupling sequence, number of scans = 32, repetition delay = 5 s, and number of t_1 increments = 128, with the increment set equal to one rotor period of 45.45 μs) (D) ^{13}C CP MAS NMR spectrum (10 kHz MAS, number of scans = 7000, repetition delay = 5 s, contact time = 2 ms, and line broadening = 80 Hz) (E) 2D CP MAS ^{1}H–^{13}C HETCOR NMR spectrum acquired with short contact times of 0.2 ms under 8.5 kHz MAS, number of scans per increment = 1500, repetition delay = 5 s, number of t_1 increments = 32, and line broadening = 80 Hz.

The ^{13}C CP MAS NMR of **2** displays three signals at 23, 67, and 85 ppm (Fig. 3D). Additionally, the 2D ^{1}H–^{13}C HETCOR NMR spectrum (Fig. 3E, short contact time of 0.2 ms) shows a correlation between the methyl protons at 1.2 and 1.4 ppm and the carbon atoms at 23 ppm, which allows the assignment of the carbon–proton pairs to the methyl groups of the two isopropoxide ligands of **2**. Furthermore, correlations are evident between the two CH methine protons at 4.3 and 5.5 ppm and the two carbon atoms at 67 and 85 ppm, respectively.

Additional off-diagonal correlations in the ^{1}H DQ and TQ NMR spectra (Fig. 3B and C) between the first spin system of CH_3 and CH (1.2 and 4.3 ppm in the single-quantum frequency; 5.5 and 6.7 ppm in indirect dimensions of the DQ and TQ spectra, respectively) and the second spin system of CH_3 and CH (1.4 and 5.5 ppm in the single-quantum frequency; 6.9 and 8.3 ppm in indirect dimensions of the DQ and TQ spectra, respectively) indicating spatial proximity of the two chemical environments.

The ^{1}H and ^{13}C CP MAS NMR spectra of **3** (Fig. 4) as the product of the gradual thermolysis of **2**, clearly show the nearly complete disappearance of the peaks at 5.5 ppm (slightly shifted to 5.8 ppm) and 85 ppm, respectively, which were present in **2** (Fig. 3A and B). Consistent with the results obtained from IR spectroscopy, and with the formation of propylene during thermal treatment, this observation suggests the removal of one kind of isopropoxide ligand from **2** upon thermolysis.

It should be noted that the two isopropoxide signals of **2** display two significantly different sets of chemical shifts, 5.5 ppm for ^{1}H NMR and 85 ppm for ^{13}C NMR, *versus* 4.3 ppm for ^{1}H NMR 67 ppm for ^{13}C NMR. The chemical difference between the two isopropoxides is evident when, upon thermal treatment of **2**, only the latter set of signals is preserved (Fig. 4). The first set of signals is compatible with a vanadium isopropoxide moiety, (V–O–C<u>H</u>$(CH_3)_2$) and (V–O–<u>C</u>H$(CH_3)_2$) respectively.[27,28] The second set of signals is attributable to a non-metal bound isopropoxide (see, for instance, the spectrum of tetraisopropyl orthosilicate (Si–O–C<u>H</u>$(CH_3)_2$): 4.2 ppm; (Si–O–<u>C</u>H$(CH_3)_2$): 65.7 ppm. AIST database, Chart: 19 429, accessed March 2018).

Considering the grafting stoichiometry for **2** of a vanadium complex per silanol, as demonstrated by elemental analysis and

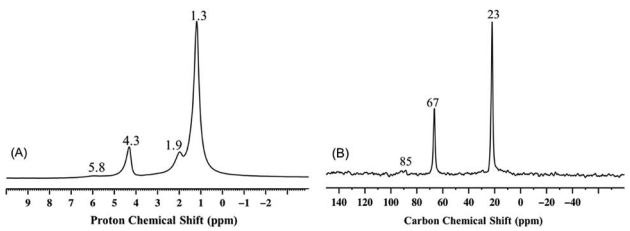

Fig. 4 Solid-state NMR of **3** obtained from the gradual thermolysis of **2** at 200 °C for 1 h under static vacuum conditions. (A) 1D ^{1}H spin-echo MAS spectra (acquired on 600 MHz NMR spectrometer under a 20 kHz MAS spinning frequency, number of scans = 32, and repetition delay = 5 s) and (B) ^{13}C CP-MAS NMR spectrum (under 10 kHz MAS spinning frequency, number of scans 14 000, repetition delay = 5 s, contact time = 2 ms, and line broadening = 80 Hz).

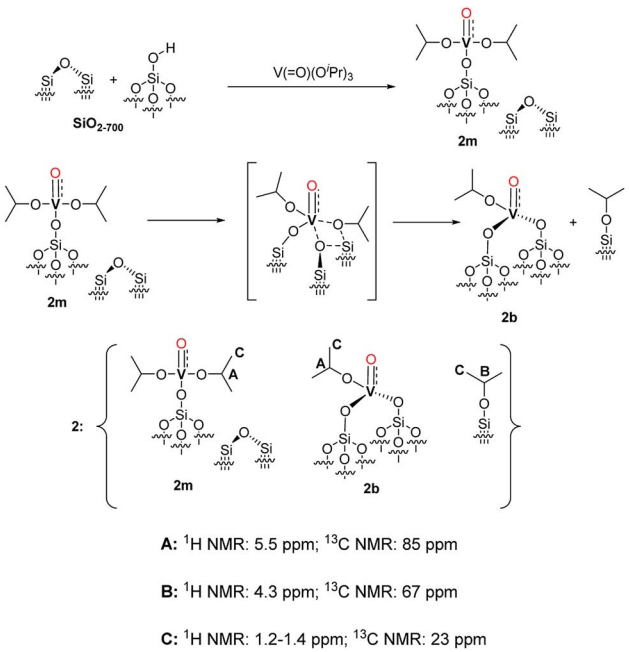

Scheme 2 Proposed structure of **2** with a monopodal [(≡Si–O–)V(O)(O^{i}Pr)$_2$] complex (**2m**), a bipodal [(≡Si–O)$_2$V(O)(O^{i}Pr)] complex (**2b**) and alkylated silanol (≡Si–O–^{i}Pr) with the assignment of the respective NMR signals. The formation pathways of **2m** and **2b** are outlined in the first and second reaction lines of the Scheme respectively. The vanadyl bond of **2m**, **2b** is reported as a triple V≡O bond according to the NBO presented in the computational section and in Fig. S5.†

FT-IR spectroscopy, an hypothesis on the identity and formation of the surface complexes in **2** can be drawn as in Scheme 2.

The initial grafting of the precursor takes place in a monopodal fashion by reaction with the isolated silanols of $SiO_{2\text{-}700}$ generating **2m**. The latter complex can, in part, react with the strained siloxane bridges present on $SiO_{2\text{-}700}$ by a metathesis reaction leading to **2b** and (≡Si–O–^{i}Pr) moieties. The ability of the strained siloxane bridges of highly dehydroxylated silica to participate in grafting reactions and in the rearrangement of surface complexes by σ-bond metathesis is known.[31,36,39] The rearrangement of **2m** to **2b** does not generate new silanol moieties in agreement with the lack of such functionalities in **2** as observed by FT-IR (Fig. 1). Further study of **2m** by DFT calculations (see the computational section for further details) demonstrated the partial triple bond character (indicated as dashed bond in Scheme 2) of the vanadyl moiety of **2m** with a bond order of 2.62 based on a natural bonding orbital (NBO) analysis of a model of **2m** (see also Fig. S5 in the ESI†). The same observation is likely to hold also for **2b**. When comparing our results to other studies on the grafting of vapors of **1** on dehydroxylated silica, Rice and Scott reported exclusively a signal at 84.3 ppm in the SS ^{13}C NMR (not shown in the original manuscript) of the grafted complex.[27] Hermans *et al.* observed a main signal at 85 ppm and a minor signal at 67 ppm. They attributed the former signal to monopodal [(≡Si–O–)V(O)(O^{i}Pr)$_2$] and the latter to a monopodal complex (**4**, Scheme 3) formed by the reaction of **1** with a strained siloxane bridge.[28]

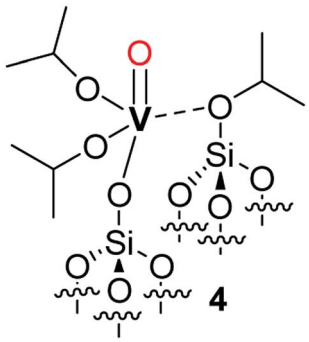

Scheme 3 Representation of complex **4** proposed by Hermans *et al.*[28] as the product of the reaction of **1** with a strained siloxane bridge.

However, this attribution does not seem in agreement with the observation by the authors that only **4** is formed when using silica supports dehydroxylated at lower temperatures that present less strained and a lower density of siloxane bridges; the formation of bipodal species would be expected when less dehydroxylated silicas are employed.[2]

In any case, it appears that the bipodal complex **2b**, to the formation of which we attribute the signal at 67 ppm ($\equiv$SiO<u>C</u>H$(CH_3)_2$), is produced in significant amounts by solution phase grafting and in negligible amounts when **1** is grafted as a vapor. Further comparison between this work and previous literature was carried out by analysis of the ^{51}V MAS NMR of the grafted complexes. The ^{51}V MAS NMR of **2** and of **2-SiO$_{2\text{-}300}$** (the complex prepared by grafting of **1** on silica dehydroxylated at 300 °C, $SiO_{2\text{-}300}$) are displayed in Fig. 5A and B respectively.

The ^{51}V MAS NMR spectra of **2** displays one resonance at −651 ppm, as determined by variation of the spinning frequency, slightly shifted from −630 ppm of precursor complex **1**.[27]

The presence of a single band may appear in disagreement with the presence of two different vanadium complexes (**2m** and **2b**) in **2**, however, as proposed by Rice and Scott,[27] the monopodal and bipodal complexes might have similar chemical shift and their resolution by ^{51}V MAS NMR might be challenging.

Hermans *et al.* could resolve two signals, at −630 ppm and −655 ppm, and they attributed the first to monopodal [($\equiv$Si–O–)V(O)($O^iPr)_2$] and the second to less symmetrical complex **4**.[28]

Based on these considerations, the resonance at −651 ppm for **2** could result from the coalescence of the signals relative to **2m** and **2b**. Indeed, a small shift to −660 ppm for **2-SiO$_{2\text{-}300}$**, that should contain predominantly bipodal species such as **2b**,[2,40] is observed compared to **2** suggesting that the bipodal species might display a slight upfield shift compared to the monopodal complexes.

Finally, when **2** was thermally treated to afford **3**, the set of signals at 5.5 and 85 ppm (see Fig. 3 and 4) disappeared whereas that at 4.3 and 67 ppm was preserved. Based on the peak assignment in Scheme 2, this transformation should correspond to the loss of the isopropoxide moieties from **2m** and **2b** with the retention of the isopropoxide of ($\equiv$Si–O–^{i}Pr). Interestingly, a temperature of 200 °C is sufficient to entirely remove the isopropoxide groups bound to vanadium. This transformation is accompanied by the appearance of a small peak at 1.9 ppm in the ^{1}H MAS NMR spectra of **3** (Fig. 4A), typically assigned to isolated $\equiv$SiOH groups, which are also present in the form of a band at 3741 cm^{-1} in the IR spectrum of **3** (Fig. 1).

The reconstruction and rearrangement of vanadium sites on silica and the formation of tripodal vanadium species under various conditions has been discussed previously.[11,12,14,28,41]

Based on the observed formation of propylene, the thermal restructuring of vanadium isopropoxide sites has been proposed to proceed *via* a γ-H transfer from the methyl group of the isopropoxide to the vanadyl oxygen producing V–OH moieties that can subsequently react with the siloxane bridges.[28] Accordingly, the evolution of **2** upon thermal treatment can be described as in Scheme 4.

The produced V–OH groups, observed in **3** by the appearance of a band at 3660 cm^{-1} in the FT-IR spectrum (Fig. 1),[36] can, in part, react with the strained siloxane bridges to generate multipodal species up to the formation of the tetrahedral VO_4 complex. The latter complexes can also be generated by the reaction of the V–OH moieties with adjacent silanol groups. The ($\equiv$Si–O–^{i}Pr) groups are preserved in **3** likely because, in the absence of C–H activation by the vanadyl group, the treatment temperature of 200 °C is not sufficient to afford the complete decomposition of these species.

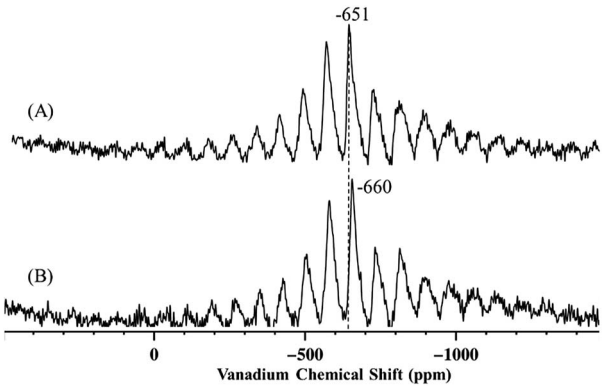

Fig. 5 ^{51}V MAS NMR as determined by variation of the spinning frequency of (A) **2** and (B) **2-SiO$_{2\text{-}300}$** (236.7 MHz, acquired on 900 MHz NMR spectrometer under a 20 KHz MAS spinning frequency, repetition delay = 0.25 s).

DFT mechanistic study

The key process for the transformation of complex **2** to **3** upon thermal treatment is the transfer of a proton of the methyl group of the isopropoxide to the vanadyl oxygen. In this section we provide deeper insight into this transformation by a DFT approach. Fig. 6 illustrates two possible reaction pathways for the abovementioned process: a concerted pathway (P1, green) and a two-step radical pathway (P2, purple).

Both pathways proceed *via* a six-membered arrangement where a methyl group from an isopropoxide ligand is placed in close vicinity to the vanadium-oxo functional group.

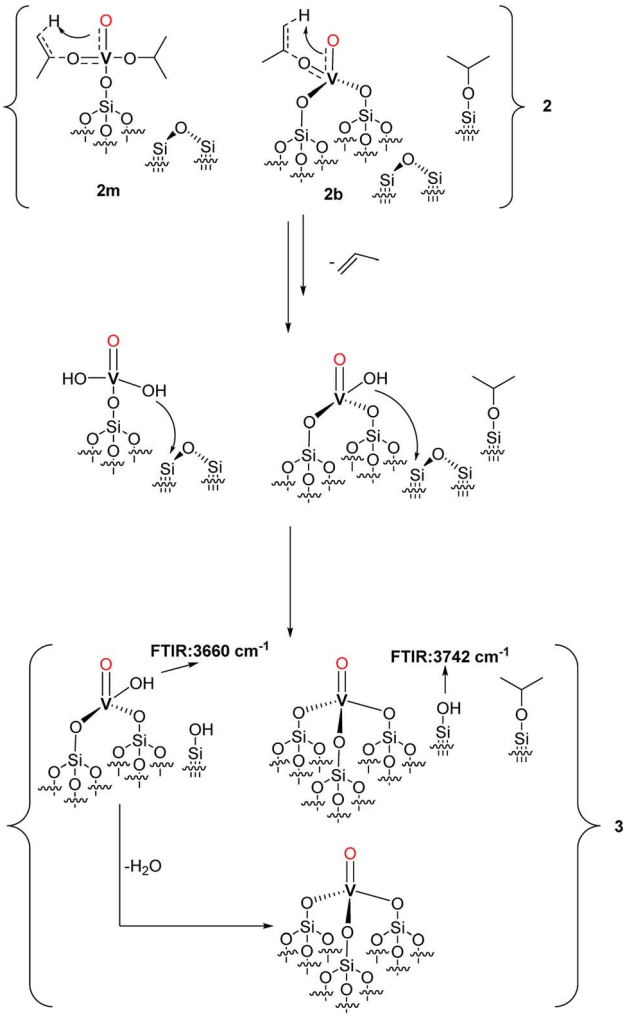

Scheme 4 Proposed surface complexes and moieties in **3** as an effect of thermal rearrangement of **2**.

The concerted pathway proceeds *via* a transition state **A**, in which both the C–H and C–O bonds of the involved isopropoxide ligand are cleaved.

The H atom is transferred to the oxygen of the vanadyl moiety, which is transformed into the V–OH group, whereas, cleavage of the O–C bond, converts the former vanadium isopropoxide moiety into a vanadium oxo moiety. At the same time, the C_α–C_β bond of the reacting isopropoxide ligand assumes a double-bond character to form a molecule of propene that is eliminated at the end of the elementary reaction step.

In this mechanism, the vanadium center is always in a formal oxidation state of +5 (d^0) and the overall reaction step occurs on the singlet spin state. The free energy barrier to access the **A** concerted transition state from the initial complex was calculated at 33.5 kcal mol^{-1}. A natural population analysis (NPA) found a charge of 0.40 e on the transferred H atom that hints at a proton transfer step. Sauer *et al.* proposed a similar step earlier in their theoretical investigation into the mechanism of oxidative dehydrogenation of propane. They reported a barrier of 38 kcal mol^{-1} for the H-transfer from one of the methyl groups of a V-bound isopropoxide to the O atom of

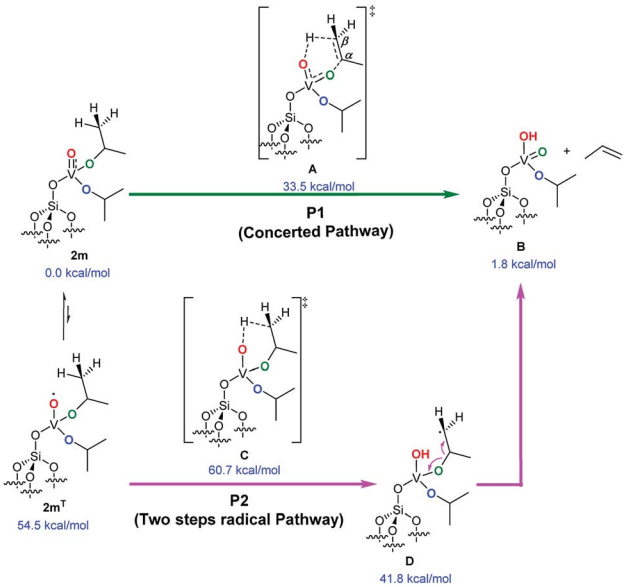

Fig. 6 DFT-based reaction mechanisms for the γ-H-transfer and elimination of propene. The concerted pathway (P1, green) is energetically favorable over the two-step radical pathway (P2, purple; see the ESI for the energy diagram).

a ≡Si–O–V moiety, with the V-metal center in the formal oxidation state of +4 (d^1).[19]

Alternatively, the two-step radical pathway is initiated by a H-transfer from one of the methyl groups of the isopropoxide ligands to the vanadium-oxo group by the **C** transition state. This leads to intermediate **D**, which has a biradical character with one spare electron located on the isopropoxide group and the other on the V-metal center with a formal oxidation state of +4 (d^1). Although the **C** transition state could exist in the triplet spin, and/or open-shell singlet states using a broken-symmetry approach, it was localized in the triplet spin state 60.7 kcal mol^{-1} above **2m**. However, the main source of this large barrier is not to be found in the H-transfer but in the change of spin state, since **2m** optimized in the triplet state, $\mathbf{2m^T}$, is 54.5 kcal mol^{-1} above **2m** in the singlet spin state. The **C** transition state collapses into intermediate **D**, shown in Fig. 6, located 41.8 kcal mol^{-1} above **2m**. Intermediate **D** has its two excess electrons located at the V-metal center and at the isopropoxide C_β atom (with a spin density of 1.03 e and 1.09 e, respectively). The energy difference between the **C** transition and the **A** transition states along the concerted pathway is 27.2 kcal mol^{-1}; which is high enough to rule out the two-step pathway on the triplet spin state. Alternatively, we were unable to localize the open-shell singlet **C** transition state using a broken-symmetry approach, the system collapsed into a four-membered closed-shell singlet (V–C–C–O, **D′**) metallacycle (not shown). Because this metallacycle lies 45.1 kcal mol^{-1} above **2m** on the singlet spin state, and because it is reached through a transition state of roughly 65 kcal mol^{-1} (**C′**, see Fig. S4† for an overview), this unlikely reaction pathway is not commented further. In conclusion, our analysis clearly indicates that propene elimination from **2m** occurs on the singlet spin state *via* the concerted pathway **A** involving a single transition state.

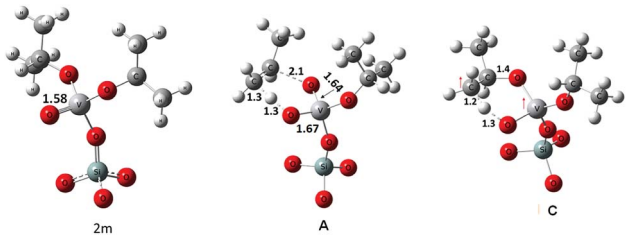

Fig. 7 Geometries of the A and C transition states (selected distances in Å).

The geometries of **2m** and of transition states, **A** and **C**, are shown in Fig. 7. In **2m** the V–O bond is calculated to be approximately 1.58 Å long suggesting a partial triple bond character[42,43] as demonstrated by the NBO analysis (see Fig. S5† for an overview). In case of transition state A the geometry of the V-center is a distorted tetrahedron. The V–O bond that is formed by the cleavage of the C–O bond has a length of 1.64 Å and a partial triple bond character (bond order: 2.48). The V–O bond receiving a proton from the methyl group of the isopropyl moiety has a length of 1.67 Å and a bond order of 1.7. The two other V–O bonds have a length of about 1.8 Å.

The geometry of **C** shows that the cleaving C–H bond and the forming O–H bond are in the range of 1.2–1.3 Å, whereas the O–C bond, that must be cleaved to release propene, is still stable at 1.43 Å. Analysis of the spin density clearly indicates that one of the two excess electrons is located on the V-atom (spin density of 1.01 e) while the other is substantially shared between the O and C atoms involved in the H-transfer (with spin densities of 0.61 e and 0.38 e respectively).

Conclusions

The grafting of vanadium oxytriisopropoxide on the surface of dehydroxylated silica was studied by the surface organometallic chemistry approach. The complexes and moieties formed on the support upon grafting and after a controlled thermal treatment were carefully characterized by elemental analysis and FTIR, SS NMR, Raman and EPR spectroscopies. It was found that the reaction of **1** with the support surface generates monopodal (**2m**) and bipodal (**2b**) complexes, the latter, likely originated by the reaction of the monopodal species with a strained siloxane bridge. The complexes generated on the surface by the thermal rearrangement of **2m** and **2b** have been discussed. DFT analysis strongly supports a mechanism where a concerted intramolecular γ-H-atom transfer from an isopropoxide ligand's methyl group to the vanadyl oxygen takes place along with the cleavage of the O-isopropyl bond to liberate propene. Overall, we believe that this work contributes to a deeper understanding of the reactivity and wet-chemistry grafting patterns of vanadium alkoxide complexes. The latter compounds can be regarded as potential models to study hydrogen-transfer steps in reaction networks related to propane dehydrogenation.

Conflicts of interest

There are no conflicts to declare.

Acknowledgements

This work was funded by King Abdullah University of Science and Technology, Thuwal, Saudi Arabia. The authors declare no competing financial interest. V. D. E. thanks the Thailand Research Fund (Grant No. RSA6080059) for funding this research.

References

1 M. Sutradhar, L. M. D. R. S. Martins, M. F. C. Guedes da Silva and A. J. L. Pombeiro, *Coord. Chem. Rev.*, 2015, **301–302**, 200–239.
2 K. C. Szeto, B. Loges, N. Merle, N. Popoff, A. Quadrelli, H. Jia, E. Berrier, A. De Mallmann, L. Delevoye, R. M. Gauvin and M. Taoufik, *Organometallics*, 2013, **32**, 6452–6460.
3 C. A. Carrero, R. Schloegl, I. E. Wachs and R. Schomaecker, *ACS Catal.*, 2014, **4**, 3357–3380.
4 P. Gruene, T. Wolfram, K. Pelzer, R. Schlögl and A. Trunschke, *Catal. Today*, 2010, **157**, 137–142.
5 A. Dinse, T. Wolfram, C. Carrero, R. Schlögl, R. Schomäcker and K. P. Dinse, *J. Phys. Chem. C*, 2013, **117**, 16921–16932.
6 M. Cavalleri, K. Hermann, A. Knop-Gericke, M. Hävecker, R. Herbert, C. Hess, A. Oestereich, J. Döbler and R. Schlögl, *J. Catal.*, 2009, **262**, 215–223.
7 N. Magg, B. Immaraporn, J. B. Giorgi, T. Schroeder, M. Bäumer, J. Döbler, Z. Wu, E. Kondratenko, M. Cherian, M. Baerns, P. C. Stair, J. Sauer and H.-J. Freund, *J. Catal.*, 2004, **226**, 88–100.
8 M. A. Bañares and I. E. Wachs, *J. Raman Spectrosc.*, 2002, **33**, 359–380.
9 J. N. J. van Lingen, O. L. J. Gijzeman, R. W. A. Havenith and J. H. van Lenthe, *J. Phys. Chem. C*, 2007, **111**, 7071–7077.
10 H. Kim, G. A. Ferguson, L. Cheng, S. A. Zygmunt, P. C. Stair and L. A. Curtiss, *J. Phys. Chem. C*, 2011, **116**, 2927–2932.
11 L. Cheng, G. A. Ferguson, S. A. Zygmunt and L. A. Curtiss, *J. Catal.*, 2013, **302**, 31–36.
12 I. E. Wachs, *Dalton Trans.*, 2013, **42**, 11762–11769.
13 H. Tian, E. I. Ross and I. E. Wachs, *J. Phys. Chem. B*, 2006, **110**, 9593–9600.
14 S. L. Wegener, H. Kim, T. J. Marks and P. C. Stair, *J. Phys. Chem. Lett.*, 2011, **2**, 170–175.
15 C. A. Carrero, C. J. Keturakis, A. Orrego, R. Schomäcker and I. E. Wachs, *Dalton Trans.*, 2013, **42**, 12644–12653.
16 J. T. Grant, C. A. Carrero, A. M. Love, R. Verel and I. Hermans, *ACS Catal.*, 2015, **5**, 5787–5793.
17 K. Alexopoulos, M.-F. Reyniers and G. B. Marin, *J. Catal.*, 2012, **289**, 127–139.
18 X. Rozanska, R. Fortrie and J. Sauer, *J. Am. Chem. Soc.*, 2014, **136**, 7751–7761.
19 X. Rozanska, R. Fortrie and J. Sauer, *J. Phys. Chem. C*, 2007, **111**, 6041–6050.
20 F. Gilardoni, A. T. Bell, A. Chakraborty and P. Boulet, *J. Phys. Chem. B*, 2000, **104**, 12250–12255.
21 H. Fu, Z.-P. Liu, Z.-H. Li, W.-N. Wang and K.-N. Fan, *J. Am. Chem. Soc.*, 2006, **128**, 11114–11123.

22 P. C. Redfern, P. Zapol, M. Sternberg, S. P. Adiga, S. A. Zygmunt and L. A. Curtiss, *J. Phys. Chem. B*, 2006, **110**, 8363–8371.
23 M.-J. Cheng, K. Chenoweth, J. Oxgaard, A. van Duin and W. A. Goddard, *J. Phys. Chem. C*, 2007, **111**, 5115–5127.
24 J. Sauer, M. Pritzsche and J. Döbler, *J. Phys. Chem. C*, 2014, **118**, 29159–29163.
25 J. Liu, F. Mohamed and J. Sauer, *J. Catal.*, 2014, **317**, 75–82.
26 R. Schlögl, Concepts in Selective Oxidation of Small Alkane Molecules, in *Modern Heterogeneous Oxidation Catalysis*, ed. N. Mizuno, Wiley-VCH Verlag GmbH & Co. KGaA, 2009, pp. 1–42.
27 G. L. Rice and S. L. Scott, *Langmuir*, 1997, **13**, 1545–1551.
28 A. M. Love, C. A. Carrero, A. Chieregato, J. T. Grant, S. Conrad, R. Verel and I. Hermans, *Chem. Mater.*, 2016, **28**, 5495–5504.
29 J. D. A. Pelletier and J.-M. Basset, *Acc. Chem. Res.*, 2016, **49**, 664–677.
30 C. Copéret, A. Comas-Vives, M. P. Conley, D. P. Estes, A. Fedorov, V. Mougel, H. Nagae, F. Núñez-Zarur and P. A. Zhizhko, *Chem. Rev.*, 2016, **116**, 323–421.
31 N. Maity, S. Barman, E. Callens, M. K. Samantaray, E. Abou-Hamad, Y. Minenkov, V. D'Elia, A. S. Hoffman, C. M. Widdifield, L. Cavallo, B. C. Gates and J.-M. Basset, *Chem. Sci.*, 2016, **7**, 1558–1568.
32 Z. S. Qureshi, A. Hamieh, S. Barman, N. Maity, M. K. Samantaray, S. Ould-Chikh, E. Abou-hamad, L. Falivene, V. D'Elia, A. Rothenberger, I. Llorens, J.-L. Hazemann and J.-M. Basset, *Inorg. Chem.*, 2017, **56**, 861–871.
33 Y. Bouhoute, A. Garron, D. Grekov, N. Merle, K. C. Szeto, A. De Mallmann, I. Del Rosal, L. Maron, G. Girard, R. M. Gauvin, L. Delevoye and M. Taoufik, *ACS Catal.*, 2014, **4**, 4232–4241.
34 N. Maity, S. Barman, Y. Minenkov, S. Ould-Chikh, E. Abou-Hamad, T. Ma, Z. S. Qureshi, L. Cavallo, V. D'Elia, B. C. Gates and J.-M. Basset, *ACS Catal.*, 2018, **8**, 2715–2729.
35 N. Maity, S. Barman, E. Abou-Hamad, V. D'Elia and J.-M. Basset, *Dalton Trans.*, 2018, **47**, 4301–4306.
36 S. Barman, N. Maity, K. Bhatte, S. Ould-Chikh, O. Dachwald, C. Haeßner, Y. Saih, E. Abou-Hamad, I. Llorens, J.-L. Hazemann, K. Köhler, V. D'Elia and J.-M. Basset, *ACS Catal.*, 2016, **6**, 5908–5921.
37 M. J. Kelly, A. Barthel, C. Maheu, O. Sodpiban, F.-B. Dega, S. V. C. Vummaleti, E. Abou-Hamad, J. D. A. Pelletier, L. Cavallo, V. D'Elia and J.-M. Basset, *J. CO2 Util.*, 2017, **20**, 243–252.
38 C. Resini, T. Montanari, G. Busca, J.-M. Jehng and I. E. Wachs, *Catal. Today*, 2005, **99**, 105–114.
39 B. Werghi, A. Bendjeriou-Sedjerari, J. Sofack-Kreutzer, A. Jedidi, E. Abou-Hamad, L. Cavallo and J.-M. Basset, *Chem. Sci.*, 2015, **6**, 5456–5465.
40 V. D'Elia, H. Dong, A. J. Rossini, C. M. Widdifield, S. V. C. Vummaleti, Y. Minenkov, A. Poater, E. Abou-Hamad, J. D. A. Pelletier, L. Cavallo, L. Emsley and J.-M. Basset, *J. Am. Chem. Soc.*, 2015, **137**, 7728–7739.
41 Z. Wu, S. Dai and S. H. Overbury, *J. Phys. Chem. C*, 2009, **114**, 412–422.
42 S. Pacigova, R. Gyepes, J. Tatiersky and M. Sivak, *Dalton Trans.*, 2008, 121–130.
43 S. DiBella, G. Lanza, A. Gulino and I. Fragala, *Inorg. Chem.*, 1996, **35**, 3885–3890.